AUTOCONVOLUTION AND PANORAMA: AUGMENTING SECOND-ORDER SIGNAL ANALYSIS

Scott C. Douglas[1,2]

[1]Southern Methodist University
[2]LGT Corporation
Dallas, Texas 75275 USA
douglas@lyle.smu.edu

Danilo P. Mandic

Imperial College London
Department of Electrical Engineering
London, SW7 2BT United Kingdom
d.mandic@imperial.ac.uk

ABSTRACT

The autocorrelation does not differentiate between deterministic and stochastic signals, as phase information is not maintained. This paper introduces the *autoconvolution* for both deterministic and stochastic signals. The autoconvolution with the autocorrelation provides a second-order description that discriminates between deterministic and stochastic signals – even those with identical power spectra. We also introduce the *panorama* as the Fourier transform of the autoconvolution. The power spectrum and panorama admit a two-dimensional spectral representation that has unique and powerful properties, such as detecting deterministic sinusoidal components in correlated stochastic noise without knowledge of the sinusoidal frequencies or amplitudes. Additional extensions are indicated.

Index Terms— autocorrelation, convolution, covariance matrices, frequency estimation, phase estimation, spectral analysis.

1. INTRODUCTION

The autocorrelation is a standard second-order tool for signal analysis. It is a one-dimensional function of time that, for both deterministic and stochastic finite-power signals $x(t)$, is given by

$$r(\tau) \;=\; \lim_{T\to\infty} \frac{1}{2T} \int_{-T}^{T} E\{x(t)x(\tau+t)\}dt, \qquad (1)$$

where $E\{\cdot\}$ denotes the statistical expectation operand. The Fourier transform of the autocorrelation is the power spectrum, $R(\omega)$ which is used in numerous applications, particularly for signals that are nearly-periodic or have a well-defined harmonic structure [1].

Being an integral transform, the autocorrelation function of $x(t)$ is not unique, and two different signals can have the same $r(\tau)$. For example, the signal $x(t) = A\delta(t-t_0)$ for any time delay t_0 has $r(\tau) = A^2\delta(\tau)$, where $\delta(\tau)$ is the Dirac unit impulse function. A zero-mean wide-sense stationary uncorrelated random process with signal power A^2 also has $r(\tau) = A^2\delta(\tau)$. This non-uniqueness is due to the phase information contained in $x(t)$ which is not represented in either $r(\tau)$ or $R(\omega)$. To further solidify this point, consider the signal $x(t) = A\cos(\omega_0 t + \phi)$, where A and ω_0 are fixed and ϕ is either a constant or a random variable with any probability density $p_\phi(\phi)$. The autocorrelation does not represent the information in ϕ, such that $r(\tau) = 0.5A^2\cos(\omega_0\tau)$ independent of the nature of ϕ.

A second-order description of $x(t)$ that maintains phase information of $x(t)$ can be constructed using a reference signal $y(t)$ and the cross-correlation function $r_{xy}(\tau)$ of $x(t)$ and $y(t)$ [1]. Cross-correlation requires the existence of the reference signal $y(t)$ that is related to $x(t)$. Any strategy of generating $y(t)$ from $x(t)$ requires user intervention, such as data partitioning, signal averaging, and/or additional processing. To our knowledge, no prior second-order description of $x(t)$ has been developed to carefully represent both deterministic and stochastic signals simultaneously, uniquely, and with regard to phase.

In this paper, we introduce a new second-order signal representation called the *autoconvolution.* The autocovolution, when combined with the autocorrelation, provides new insight into signals containing both deterministic and stochastic components. In particular, the autoconvolution of a wide-sense stationary random process with a finite-energy autocorrelation is zero, and thus the autoconvolution retains information about the deterministic components only. Moreover, we introduce the *panorama* as the Fourier transform of the autoconvolution. Combining the power spectrum and panorama within a two-dimensional matrix representation, a number of useful results are obtained. In particular, we demonstrate that an eigenanalysis of this matrix as a function of frequency identifies the presence of sinusoidal components obscured by random noise, even in situations where the noise is correlated and thus exhibits peaks in its power spectrum.

2. THE AUTOCONVOLUTION

For a finite-power signal $x(t)$ containing both deterministic and stochastic components, the autoconvolution of $x(t)$ is de-

978-1-4799-2893-4/14/$31.00 ©2014 IEEE

fined as

$$p(\tau) \quad = \quad \lim_{T\to\infty} \frac{1}{2T} \int_{-T}^{T} E\{x(t)x(\tau - t)\}dt. \qquad (2)$$

Comparing (2) with (1), we see that the difference is a negative sign on the integration argument within the second signal of the integration. In the limit at $T \to \infty$, $p(\tau)$ is the expected value of the convolution of $x(t)$ with itself. The expectation $E\{\cdot\}$ assumes that the joint p.d.f. $p_{x(t_1),x(t_2)}(x_1, x_2)$ exists for any pair (t_1, t_2).

The autoconvolution behaves differently than the autocorrelation for deterministic signals and wide-sense stationary stochastic signals, respectively. The following theorems indicates this fact, the proofs of which are omitted for brevity.

Theorem 1.1: For a wide-sense stationary random process $x(t)$ with a finite-energy autocorrelation function such that

$$\int_{-\infty}^{\infty} |r(\tau)|d\tau \quad < \quad \infty \qquad (3)$$

the autconvolution $p(\tau)$ of $x(t)$ is zero.

Theorem 1.2: Consider a deterministic signal $x(t)$ consisting of a sum of sinusoids of the form

$$x(t) \quad = \quad \sum_{n=1}^{N} A_n \cos(\omega_n t + \phi_n) \qquad (4)$$

where the triple $\{A_n, \omega_n, \phi_n\}$ denote the { amplitude, frequency, phase } of each sinusoidal component. Then, the autocorrelation and autoconvolution of $x(t)$ are

$$r(\tau) \quad = \quad \sum_{n=1}^{N} \frac{A_n^2}{2} \cos(\omega_n \tau) \qquad (5)$$

$$p(\tau) \quad = \quad \sum_{n=1}^{N} \frac{A_n^2}{2} \cos(\omega_n \tau + 2\phi_n). \qquad (6)$$

Remark 1: The above results already indicate one useful application of the autoconvolution: it produces a signal that encodes the amplitudes, frequencies, and phases of a sum of sinusoids while effectively removing any stochastic noise component that may be present in $x(t)$.

Remark 2: Taken together, $r(\tau)$ and $p(\tau)$ provide a two-dimensional second-order characterization of $x(t)$. Although vector notation could be used, we are motivated by reasons to become clear shortly to place these quantities in a (2×2) *power signal matrix*

$$\mathbf{R}(\tau) \quad = \quad \begin{bmatrix} r(\tau) & p(\tau) \\ p(-\tau) & r(\tau) \end{bmatrix}. \qquad (7)$$

When $x(t)$ is wide-sense stationary with finite energy autocorrelation, we have $\mathbf{R}(\tau) = r(\tau)\mathbf{I}$, whereas for a deterministic sum-of-sinusoids, $\mathbf{R}(\tau)$ will have four non-zero entries in general.

3. THE PANORAMA

The autocorrelation forms the basis for spectral analysis through the Fourier transform, yielding the power spectrum

$$R(\omega) \quad = \quad \int_{-\infty}^{\infty} r(\tau) e^{-j\omega\tau} d\tau. \qquad (8)$$

Since the autoconvolution $p(\tau)$ is also a function of time, we define the *panorama* $P(\omega)$ of $x(t)$ as the Fourier transform of $p(\tau)$, or

$$P(\omega) \quad = \quad \int_{-\infty}^{\infty} p(\tau) e^{-j\omega\tau} d\tau. \qquad (9)$$

Due to $r(\tau)$ being real-valued and even symmetric, $R(\omega)$ is Hermitian symmetric. The panorama $P(\omega)$, however, does not possess such symmetry properties.

The Fourier transform of the power signal matrix $\mathbf{R}(\tau)$ is termed the *power spectrum matrix* and has the form

$$\mathbf{S}(\omega) = \begin{bmatrix} R(\omega) & P(\omega) \\ P(-\omega) & R(\omega) \end{bmatrix} = \begin{bmatrix} R(\omega) & P(\omega) \\ P^*(\omega) & R(\omega) \end{bmatrix}, \qquad (10)$$

where the last part of (10) follows because $x(t)$ is real-valued.

Remark 3: The form of (10) is identical to the augmented covariance matrix used to characterize non-circular random signals in complex-valued signal processing applications [2]–[13]. Thus, for real-valued signals, the power spectrum measures the covariance of the signal in the frequency domain, and the panorama measures the pseudo-covariance of the signal in the frequency domain. Signals that are wide-sense stationary have Fourier components that are circular, whereas signals that are deterministic have Fourier components that are highly non-circular. The following theorem illustrates the utility of this statement.

Theorem 2.1: Consider the signal containing a sum of deterministic sinusoidal components corrupted by random noise,

$$x(t) \quad = \quad \eta(t) + \sum_{n=1}^{\infty} A_n \cos(\omega_n t + \phi_n), \qquad (11)$$

where $\eta(t)$ is a wide-sense stationary random process with power spectrum $|H(\omega)|^2$, such that $\int_{-\infty}^{\infty} |H(\omega)|^2 d\omega < \infty$. Then, the power spectrum matrix is given by

$$\begin{aligned} \mathbf{S}(\omega) \quad = \quad & |H(\omega)|^2 \mathbf{I} \\ & + \sum_{n=1}^{\infty} \frac{A_n^2}{4} \left(\delta(\omega - \omega_n) \begin{bmatrix} 1 \\ e^{-j2\phi_n} \end{bmatrix} \begin{bmatrix} 1 & e^{j2\phi_n} \end{bmatrix} \right. \\ & \left. + \delta(\omega + \omega_n) \begin{bmatrix} 1 \\ e^{j2\phi_n} \end{bmatrix} \begin{bmatrix} 1 & e^{-j2\phi_n} \end{bmatrix} \right) \qquad (12) \end{aligned}$$

Corollary 2.1: Consider an small bandwidth B containing only one sinusoidal component with frequency ω_i in $x(t)$, and

let $\mathbf{S}_B(\omega_n)$ be the corresponding power spectrum matrix integrated over the bandwidth $(\omega_n - 0.5B, \omega_n + 0.5B)$ containing ω_i. Then,

$$\mathbf{S}_B(\omega_n) = \begin{bmatrix} \frac{A_i^2}{4} + H_{ave}(\omega_n)B & \frac{A_i^2}{4}e^{j2\phi_i} \\ \frac{A_i^2}{4}e^{-j2\phi_i} & \frac{A_i^2}{4} + H_{ave}(\omega_n)B \end{bmatrix}, \quad (13)$$

which has eigenvalues equal to

$$\lambda_{B,max}(\omega_n) = \frac{A_i^2}{2} + H_{ave}(\omega_i)B \quad (14)$$

$$\lambda_{B,min}(\omega_n) = H_{ave}(\omega_n)B \quad (15)$$

and a principal eigenvector of

$$\mathbf{q}_{B,max}(\omega_n) = \frac{1}{\sqrt{2}}[1 \quad e^{-j2\phi_i}]^T, \quad (16)$$

where $H_{ave}(\omega_n)$ is the average value of the noise spectrum within the small bandwidth. At other frequencies ω_n that do not lie near a sinusoidal frequency ω_i, $\mathbf{S}_B(\omega_n)$ is diagonal and equal to $H_{ave}(\omega_n)B\mathbf{I}$.

Remark 4: The above theorem and corollary indicate that narrowband filtering can be used to detect sinusoids in broadband noise using the eigenstructure of the power spectrum matrix alone. If the bandwidth B near a selected frequency ω_n is chosen to be small such that $H_{ave}(\omega_n)B \ll 0.5A_i^2$, then the matrix $\mathbf{S}_B(\omega_n)$ will be close to singular, indicating the presence of a sinusoidal component. At other frequencies, the matrix $\mathbf{S}_B(\omega_n)$ will be diagonal. Numerical simulations in the next section verify these claims. Moreover, the eigenvector $\mathbf{q}_{B,max}(\omega_n)$ can potentially be used to estimate the relative phases of the sinusoidal component up to a sign change, as a quadratic function of any signal cannot estimate absolute signal polarity, although this capability is still under investigation. These results make use of the *bandwidth noncircularity* $N_B(\omega_n)$ defined as

$$N_B(\omega_n) = \frac{\lambda_{B,min}(\omega_n)}{\lambda_{B,max}(\omega_n)}, \quad (17)$$

which, under the assumptions above, will have the value

$$N_B(\omega_n) = \begin{cases} \left(1 + \frac{A_n^2}{2B|H(\omega_n)|^2}\right)^{-1}, & \text{if a sinusoid is present.} \\ 1, & \text{otherwise.} \end{cases} \quad (18)$$

4. NUMERICAL SIMULATIONS

We explore the use of the autoconvolution and panorama via numerical simulations using the following procedure:

1. Form the autocorrelation $r(\tau)$ and autoconvolution $p(\tau)$ by suitable ensemble averaging.

2. Calculate the spectrum $R(\omega)$ and pseudo-spectrum $P(\omega)$ via Fourier transforms.

3. Over bands of constant bandwidth B and different center frequencies ω_n, estimate the (2×2) matrix $\mathbf{S}_B(\omega_n)$. Compute the eigendecomposition of this matrix in each band, and find the bandwidth noncircularity $N_B(\omega_n)$.

4. Where there is a strong local minimum in $N_B(\omega_n)$ as a function of ω_n, we detect the presence of a sinusoidal component.

In this case, we use discrete-time signals and employ sampled versions of the autocorrelation, autoconvolution, and Fourier transform.

We explore the above process via simulation in the discrete-time domain. Let $x(k)$ be defined as

$$x(k) = \cos(2\pi 0.15k - \pi/6) + 0.25\cos(2\pi 0.25k + \pi/3) + 0.1\cos(2\pi 0.4k + \pi/8) + \eta(k), \quad (19)$$

where $\eta(k)$ is a zero-mean Gaussian random process generated by filtering a zero-mean uncorrelated Gaussian random process with a digital filter whose system function is

$$H(z) = \frac{1}{1 - 1.8\cos(2\pi 0.2)z^{-1} + 0.64z^{-2}} \quad (20)$$

The discrete-time power spectrum of $\eta(k)$ has a peak at $\omega = 0.2$ rad/sample. We generate 100 sequences of $x(k)$ for 1000 samples each, and form ensemble-averaged autocorrelation and autoconvolution sequences from them, using a Hamming window of length 200 samples.

Fig. 1 shows the autocorrelation (top) and autoconvolution (bottom) sequences, respectively. Note that the autocorrelation sequence has a sharp peak at $k = 0$ due to the noise sequence, whereas the autoconvolution sequence does not.

The top of Fig. 2 shows the power spectrum and the absolute value of the panorama, calculated as the fast Fourier transform of the autocorrelation and autoconvolution sequences shown in Fig. 1, respectively, where a normalized frequency axis $f = \omega/\pi$ is used. The power spectrum shows three small local peaks at $\omega/\pi = \{0.3, 0.5, 0.8\}$ corresponding to the digital frequencies of the sinusoids in $x(n)$, as well as a peak at $\omega/\pi = 0.4$ due to the Gaussian noise spectrum. It would be challenging to use the power spectrum alone to identify both the presence of the sinusoids and their frequencies due to the complicated shape of $R(\omega)$. The absolute value of the panorama $|P(\omega)|$ rejects the uncorrelated Gaussian noise component, and the sinusoidal peaks are more well-defined.

The bottom of Fig. 2 shows the bandwidth noncircularity $N_B(\omega)$ computed using the (2×2) eigendecomposition of the complex-valued power spectrum matrix at each frequency bin. This function lies between zero and one, and the local minima of this function indicate the presence and frequencies of sinusoids in the signal under test. The exact position of these minima depends on the gridding used to compute the

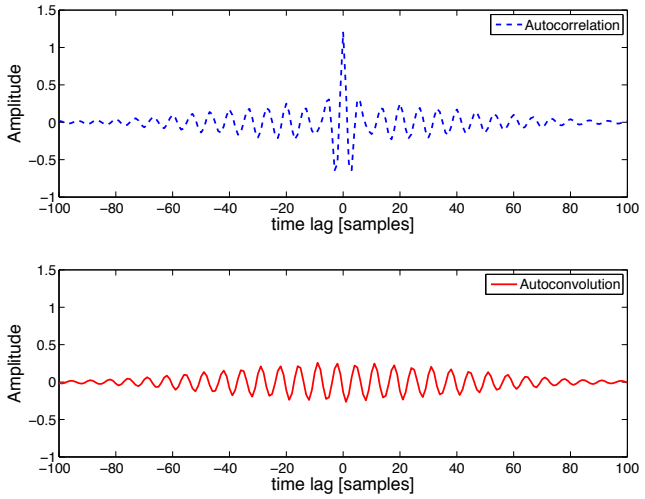

Fig. 1. Numerical estimates of the autocorrelation (top) and autoconvolution (bottom) for the discrete-time signals in the example.

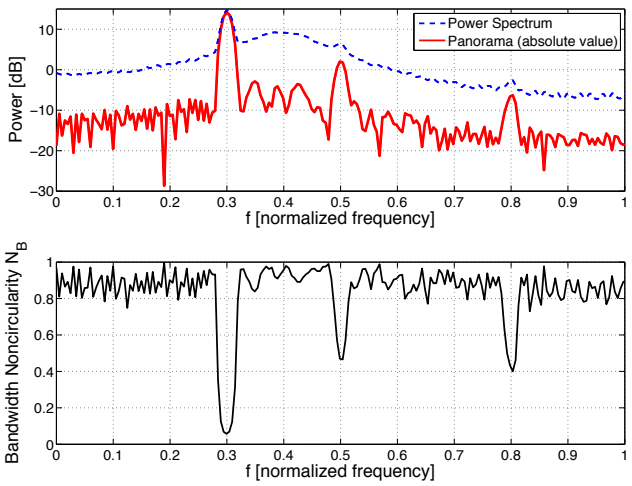

Fig. 2. Numerical estimates of the power spectrum and panorama (top) and the bandwidth noncircularity (bottom) for the discrete-time signals in the example.

power spectra and may be shifted slightly from the true sinusoidal frequencies due to numerical effects.

5. COMPUTING THE AUTOCONVOLUTION AND PANORAMA

Numerical estimates of the autocorrelation function are often computed using time averages, making use of an assumed *ergodicity property* of the signals under analysis which for stochastic signals is the assumption that the joint signal p.d.f. obeys the property $p_{t_1,t_2}(x(t_1), x(t_2)) = p_{t_1-t_2,0}(x(t_1 - t_2)x(0))$. For deterministic signals, employing time averages to compute the autocorrelation function implies that the exact phase of the signal is unknown.

It is important to note that, even in situations where a signal being analyzed is ergodic, *time averages cannot be used in place of ensemble averages* to compute its autoconvolution and/or the panorama. The reason for this limitation is due to the form of the expectation in the definition of $p(\tau)$ in (2). For stochastic signals, this expectation cannot make use of the ergodicity property. Thus, ensemble averages are required to compute the novel quantities described in this paper.

Despite its requirement for the use of ensemble averaging, the autoconvolution and panorama are expected to be useful in situations where a precise time reference exists. For digital communication tasks, this timing information might come from the physical scenario or through information in a side communications channel. Other applications where precise timing information is often available include biology, where recordings are often taken due to a stimulus injected at a precise time, and seismology, where shot records are measured using a precisely-timed acoustic disturbance.

6. CONCLUSIONS

In this paper, we have described a useful way to augment the autocorrelation of a signal. The autoconvolution together with the autoconvolution provides the information necessary to identify the deterministic and stochastic components in a generalized second-order signal analysis. The panorama is the Fourier transform of the autoconvolution. The panorama together with the power spectrum provides a way to recognize deterministic frequency components of a signal buried in random noise using a complex-valued power spectrum matrix. The relationships between the proposed signal representation and the second-order representations of complex-valued signals are the subject of current research.

7. REFERENCES

[1] S.M. Kay, *Modern Spectral Estimation: Theory and Application* (Englewood Cliffs, NJ: Prentice-Hall, 1988).

[2] B. Picinbono and P. Chevalier, "Widely linear estimation with complex data," *IEEE Trans. Signal Processing,* vol. 43, no. 8, pp. 2030-2033, Aug. 1995.

[3] B. Picinbono and P. Bondon, "Second-order statistics of complex signals," *IEEE Trans. Signal Processing,* vol. 45, no. 2, pp.411-420, Feb. 1997.

[4] R. Schober, W.H. Gerstacker, and L.H.-J. Lampe, "Data-aided and blind stochastic gradient algorithms for widely linear MMSE MAI suppression for DS-CDMA," *IEEE Trans. Signal Processing,* vol. 52, no. 3, pp.746-756, Mar. 2004.

[5] J.P. Delmas, "Asymptotically minimum variance second-order estimation for noncircular signals with application to DOA estimation," *IEEE Trans. Signal Processing,* vol. 52, no. 5, pp.1235-1241, May 2004.

[6] J. Eriksson and V. Koivunen, "Complex random vectors and ICA models: Identifiability, uniqueness, and separability," *IEEE Trans. Inform. Theory,* vol. 52, no. 3, pp. 1017-1029, Mar. 2006.

[7] P.J. Schreier, L.L. Scharf, and A. Hanssen, "A generalized likelihood ratio test for impropriety of complex signals," *IEEE Signal Processing Lett.,* vol. 13, no. 7, pp.433-436, July 2006.

[8] S.C. Douglas, "Fixed-point algorithms for the blind separation of arbitrary complex-valued non-Gaussian signal mixtures," *EURASIP Journal on Applied Signal Processing,* vol. 2007, no. 1, ID 036525, Jan. 2007.

[9] M. Novey and T. Adali, "Complex ICA by negentropy maximization," *IEEE Trans. Neural Networks,* vol. 19, no. 4, pp.596-609, Apr. 2008.

[10] S.C. Douglas and D.P. Mandic, Mean and mean-square analysis of the complex LMS algorithm for non-circular Gaussian signals," *Proc. IEEE 13th Digital Signal Processing Workshop and 5th Signal Processing Education Workshop,* Ft. Myers, FL, pp. 101-106, Jan. 2009.

[11] D.P. Mandic , S. Javidi , S.L. Goh , A. Kuh and K. Aihara, "Complex-valued prediction of wind profile using augmented complex statistics," *Renewabe Energy,* vol. 34, pp.196-201, 2009.

[12] D.P. Mandic and V.S.L. Goh, *Complex Valued Nonlinear Adaptive Filters: Noncircularity, Widely Linear and Neural Models,* (London: Wiley, 2009).

[13] Y. Xia, S.C. Douglas, and D.P. Mandic, "Adaptive frequency estimation in smart grid applications: Exploiting noncircularity and widely linear adaptive estimators," *IEEE Signal Processing Mag.,* vol. 29, no. 5, pp. 44-54, Sept. 2012.